Studies of lithium deposition and D retention on tungsten samples exposed to Li-seeded plasmas in PISCES-A

2017 Plasma Phys. Control. Fusion 59 044006

(http://iopscience.iop.org/0741-3335/59/4/044006)

IOP Publishing Plasma Physics and Controlled Fusion
Plasma Phys. Control. Fusion **59** (2017) 044006 (7pp) https://doi.org/10.1088/1361-6587/aa5bae

Studies of lithium deposition and D retention on tungsten samples exposed to Li-seeded plasmas in PISCES-A

F L Tabarés[1], D Alegre[1,2], M Baldwin[3], D Nishijima[3], M Simmonds[3], R Doerner[3], E Alves[4] and R Mateus[4]

[1] Laboratorio Nacional de Fusion, Ciemat, Avenida Complutense 22, E-28040 Madrid, Spain
[2] Fundación UNED.C/Guzman el Bueno, 133, E-28003 Madrid, Spain
[3] Centre for Energy Research, University of California at San Diego, Gilman Drive 9500, San Diego, United States of America
[4] Instituto Superior Técnico (IST), Universidade de Lisboa. Estrada Nacional N° 10, km 139, 7, 2695-066 Bobadela, Portugal

E-mail: tabares@ciemat.es

Received 17 December 2016, revised 10 January 2017
Accepted for publication 24 January 2017
Published 22 February 2017

Abstract

The interaction between lithium-seeded deuterium plasmas and tungsten targets has been studied in the PISCES-A divertor plasma simulator. Tungsten samples, of ITER-grade, with a diameter of 25 and 2 mm thick, were held at temperatures ranging from 403 to 873 K and exposed to Li/D plasmas under different plasma conditions and fixed total fluences of 5×10^{25} m^{-2}, with typical particle flux values of (1–5) $\times$ 10^{22} m^{-2} s^{-1}. The deuterium and lithium contents of the samples after irradiation were analyzed by thermal desorption spectroscopy and nuclear reaction analysis (NRA). No lithium deposition was found within the sensitivity range of NRA, except for the cold (403 K) sample on which a layer with Li atomic density below 2×10^{22} m^{-2} was detected. Deuterium retention values in the range of 10^{18} m^{-2} were measured, even for the Li deposition conditions.

Keywords: plasma facing components, liquid metals, fusion reactor, redeposition, hydrogen retention, divertor, first wall

(Some figures may appear in colour only in the online journal)

1. Introduction

The use of liquid metals as plasma facing components (PFCs) in a future fusion reactor has been proposed as an alternative to solid metals, such as tungsten and molybdenum among others [1]. The expected advantages for the power exhaust issues, mainly arising at the divertor target at power densities of 10–20 MW m^{-2}, relay on the self-healing properties of liquid surfaces as well as the ability to *in situ* replacement of the surfaces exposed to the plasma [2]. At present, three possible candidates are being explored: lithium, tin and lithium–tin alloy. While lithium is by far the best-known one and several fusion devices are already working with this metal as PFC [3], concerns about tritium retention and high vapor pressure leading to plasma dilution in the core still exist. Even when there is ample evidence of lithium hydride decomposition and fuel retention values of a few % at temperatures above 673 K [4], migration of Li from the divertor to the reactor first wall (FW) may lead to the formation of a redeposited layer of this material of potential deleterious implications for its operation, as it has been shown for carbon-based divertor targets [5]. In this context, it is important to characterize the film formation and associated D retention properties of W surfaces exposed to lithium-contaminated plasmas under conditions resembling those expected in a reactor, with FW temperatures up to 873 K and particle fluxes in the divertor strike point up to 10^{23} m^{-2} s^{-1}.

The organization of the paper is as follows. Section 2 describes the experimental set-up used in the present studies, of which the results are described in section 3. In section 4 the

Table 1. Sumary of experimental conditions.

Sample #	Exposure time (s)	Total fluence (m^{-2})	T oven (K)	Te (eV)	Ne (m^{-3})
1	900	5, 04e + 25	313	9	4, 4e + 18
2	900	3, 87e + 25	653	12	2, 9e + 18
3	900	4, 95e + 25	654	12, 5	3, 6e + 18
4	900	5, 04e + 25	675	11, 5	4e + 18
5	900	4, 05e + 25	656	10	3e + 18
6	1800	3, 42e + 25	649	14	1, 1e + 18

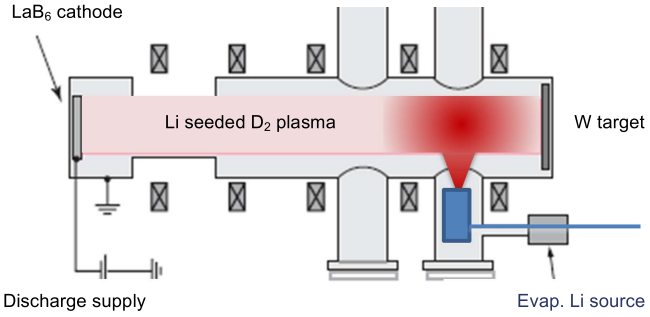

Figure 1. Sketch of the PISCES a set-up used in the experiments.

results are discussed and their implication in the integration of liquid metal based reactors with a solid metal FW are addressed.

2. Experimental set-up

The experiments were performed in the PISCES-A linear plasma device [6], able to deliver particle fluxes up to $10^{23}\,m^{-2}\,s^{-1}$ and plasma parameters similar to those expected in the divertor region of a fusion reactor ($ne < 5 \times 10^{19}\,m^{-3}$ and $Te < 10\,eV$) [7]. The machine was run in deuterium plasmas under typical conditions (see table 1) and exposures corresponding to a total dose of $5 \times 10^{25}\,m^{-2}$, implying plasma pulse durations of ~1000 s, were attained. An effusive oven provided with a circular hole of $\phi = 1$ cm at the top, was installed in the middle of the vacuum chamber, 10 cm below the plasma equatorial plane. It was filled with metallic lithium and resistively heated up to 723 K. A thermocouple was embedded into the lithium piece to guarantee a reliable reading of the temperature. This was verified by checking the reading at the well-known melting temperature of Li at 453 K and associated 'shoulder' in the temperature versus time graph. Optical emission spectroscopy (Ocean Optics USB4000 spectrometer) was used tomonitor the actual concentration of Li in the plasma. Lines at 671 and 610 nm (LiI) and 656 nm ($D\alpha$) were systematically recorded at fixed intervals in the middle of the plasma column, above the lithium oven. Reciprocating Langmuir probes were also inserted in the same location for ne and Te evaluation. Figure 1 shows a sketch of the set-up.

ITER-grade tungsten discs (Midwest Tungsten Co. $\phi = 1$ inch, 2 mm thick) were used as target. They were outgassed at 1273 K prior to their use in the experiments, except for sample #1. Their temperature during the plasma exposure was varied by controlling the thermal contact with the copper holder and forced air-cooling. In this way, the range from 403 K (maximum cooling) to 873 K could be explored. Samples were fixed to the copper holder by using a Mo cap, leading to an effective plasma-exposed area of 4 cm^2. Under most conditions, a bias of $V = -80$ V was applied to the target, but some runs at floating potential were also included. A summary of the experimental conditions is presented in table 1.

Each sample was weighed before and after the plasma exposure in a scale with 10^{-5} g resolution. Three measurements were taken each time and and the readings averaged. After exposure to the plasma, the samples were split in two and one of the halves (stored in argon gas) was sent to the IST, Lisbon, for nuclear reaction analysis (NRA) characterization. The other half was introduced into a thermal desorption spectroscopy (TDS) chamber and outgassed. Two mass spectrometers (A 0–6 u MKS microvision plus, and a SRS 100 u RGA) were used for characterizing the released gas. The SRS system detects He + D_2 together at 4 u, the MKS system is able to discriminate them, so that independent recordings of each species were possible. Thermal ramps up to 1100 K at a heating rate of 0.5 K s^{-1} were employed for the TDS analysis.

NRA was carried out at the IST of the University of Lisbon. It was performed by using 1 and 1.5 MeV ^{3}He ion beams, being the Li and ^{2}H content quantification from the $^2H(p_0)$ and $^7Li(p_0)$ proton emission yields induced by the $^2H(^3He, p)^4He$ and $^7Li(^3He, p)^9Be$ nuclear reactions. Due to the large plasma exposure area of the samples, they were analyzed in two different locations.

3. Results

3.1. Plasma composition

Before starting the systematic scans on target temperature and plasma conditions, a calibration of the Li line at 671 versus the nominal oven temperature was performed. Figure 2(a) shows a typical spectrum in the wavelength range of interest. As it can be seen, intense 671 and 656 nm peaks were detected, together with a much smaller peak at 610 nm. As expected, no emission of the LiII at 548.5 nm can be seen, since it would require excitation energies above 61.2 eV not available for our typical Te = 10 eV plasmas.

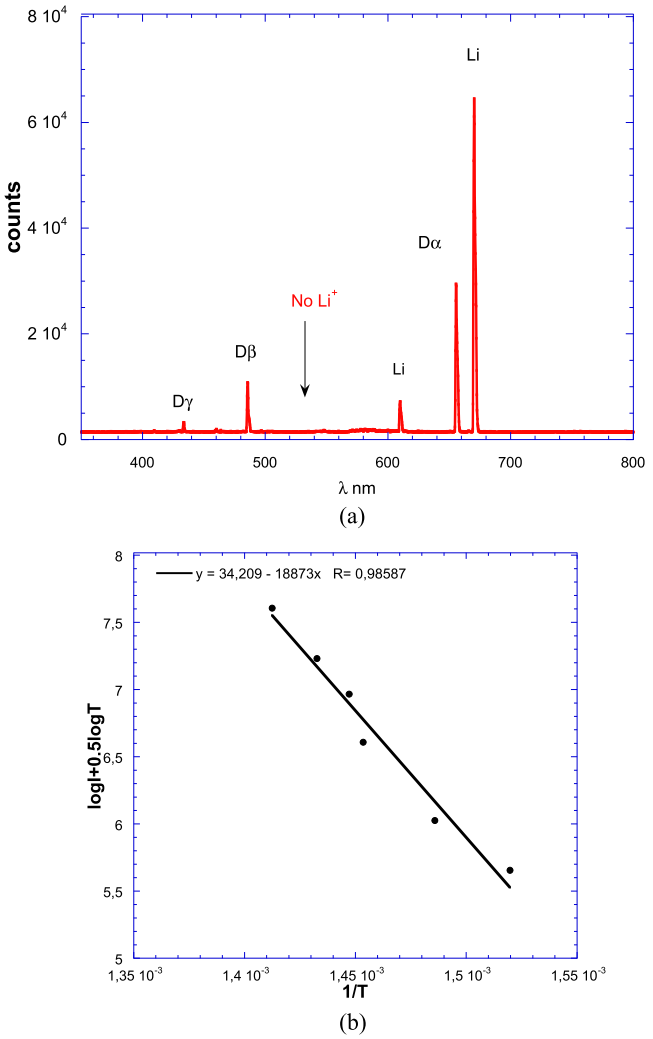

Figure 2. (a) Spectrum of a typical Li-seeded plasma. (b) Fitting of the Li intensity to expression given by equation (2). Temperatures were corrected by a 35 K offset.

The vapor pressure of lithium is given by [8]

$$P_{\mathrm{vap}}\,(\mathrm{Pa}) = 133.3 \times 10^{(18.4-18750/T)} \qquad (1)$$

with T in K, and the associated (effusive) vapor flow detected through the emission of Li in the plasma at constant ne and Te values is

$$I_{\mathrm{Li}} \sim \Gamma_{\mathrm{vap}} = \tfrac{1}{4} n_{\mathrm{Li}}.\ v_{\mathrm{Li}} = A.\ P_{\mathrm{vap}}(T).\ T^{-1/2}. \qquad (2)$$

Therefore, a plot of $\log I_{\mathrm{Li}} + 0.5 \log(T)$ versus $1/T$ should yield a straight line with slope $m = -18\,750$. When the intensity of the 671 nm line is plotted versus the recorded oven temperature in the form indicated in equation (2), the behavior displayed in figure 2(b) is obtained. In the plot, a 35 K offset has been applied to the temperature values as noted by the temperature–time characteristics of the evaporation oven on passing through the melting point of Li. From the linear fitting of the data a slope of $m = -18\,873$ is deduced, very close to the nominal value.

The concentration of the seeded impurity on the deuterium plasma in PISCES has been formerly evaluated through the absolute intensity of the respective atomic emission lines,

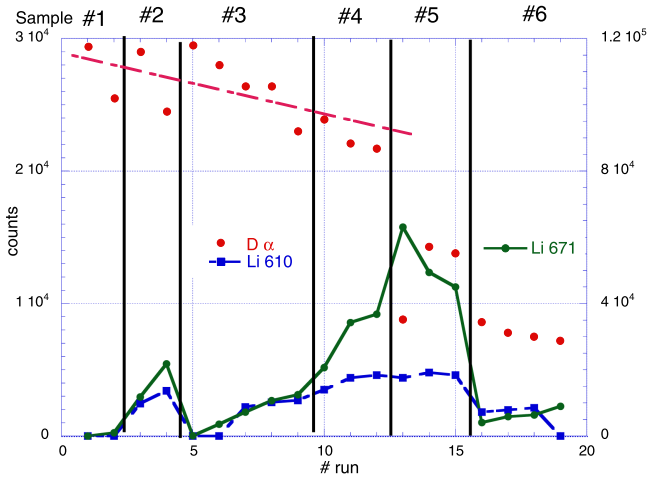

Figure 3. Summary of spectroscopic results. The sample number corresponding to the spectroscopic run is shown on the top of the figure.

LiI, at 671 and 610 nm in the present case, as previously reported for other seeded plasmas [9]. Unfortunately, no absolute calibration of the detection system was available in the present experiments, so that only raw values of the line intensities during sequential runs of the spectrometer are shown on figure 3. The corresponding sample number is also displayed on the top of the figure. As it can be seen, a slowly decaying Dα signal is observed for runs up to #13. Since fairly constant plasma parameters were deduced for the Langmuir probe data, gradual contamination of the observation window by the evaporated lithium is likely responsible for this decay. A lower level of Dα signal and a concomitant increase of the Li line is seen during sample #5 exposure, corresponding to an increase in the oven´s temperature and hence a higher Li influx. Finally, a lower plasma density was intentionally achieved during exposure of sample #6 in order to avoid excessive heating of the target.

Assuming a full ionization of the injected lithium in the plasma column (see below), simple geometrical considerations can be applied to get an estimate of the plasma composition. Thus, for an effusive source a cosine distribution of the lithium flow from the oven can be expected. For $T = 700$ K, application of equations (1) and (2) yields and effusive flux of $10^{21}\,\mathrm{m^{-2}\,s^{-1}}$. Taking into account the area of the oven's hole (1 $\mathrm{cm^2}$) and the distance to the plasma column (6 cm for a plasma radius of 4 cm), integration of the flux over the plasma projected area yields a lithium influx of $\sim 1 \times 10^{15}\,\mathrm{s^{-1}}$.

3.2. Lithium deposition

Two different diagnostics were used for the detection of a possible lithium film deposited on the W target. The samples were weighed before and after their exposure to the plasma, then split and one of the sample halves sent for NRA analysis as described in the previous section. While the first method provides an accuracy of $\sim 10^{-5}\,\mathrm{g}\ /4\,\mathrm{cm^{-2}} = 2.5 \times 10^{-6}\,\mathrm{g\,cm^{-2}}$, NRA can detect surface densities above $\sim 1 \times 10^{17}\,\mathrm{at\,m^{-2}}$, i.e., $1.17 \times 10^{-6}\,\mathrm{g\,cm^{-2}}$ for the case of lithium. Table 2 shows the results of both diagnostics for the six runs. As seen, no lithium

Table 2. Summary of results.

Exp.	T_W (K)	Bias (V)	T_{oven} (K)	TDS (D m^{-2})	TDS (He m^{-2})	Mass (Li m^{-2})	NRA(D m^{-2})	NRA (Li m^{-2})
W-Li-1	673	−80	313	8.10E + 18	7.70E + 18	0	1.20E + 20	<1.0E + 21
W-Li-2	673	−80	653	2.60E + 18	4.70E + 18	0	<1.0E + 19	<1.0E + 21
W-Li-3	873	−80	654	6.50E + 17	1.10E + 19	0	<1.0E + 19	<1.0E + 21
W-Li-4	673	−80	675	7.30E + 17	6.60E + 18	0	<1.0E + 19	<1.0E + 21
W-Li-5	673	Float	656	1.70E + 18	8.90E + 16	0	<1.0E + 19	<1.0E + 21
W-Li-6	403	Float	649	2.90E + 18	1.30E + 17	1.09E + 23	5.00E + 18[a]	1.60E + 22

[a] Higher integration time in NRA.

was detected by NRA except for sample #6, held at 403 K during the plasma exposure. The detected amount, $1.6 \times 10^{18}\,cm^{-2}$, translates into ~75 μg for a 4 cm^2 sample. This is ~6 times lower than the value deduced from weigh gain analysis. However, it must be pointed out that the very hygroscopic characteristics of lithium films [10] may lead to an overestimate of the weigh gain if exposed to the air. Furthermore, a very inhomogeneous deposition pattern was visually observed in the sample, displayed in figure 4, making a quantitative comparison even more difficult.

3.3. D retention

Again, two methods were used for the estimate of D retention on the W samples. Half of the sample was outgassed under vacuum in a devoted TDS facility. The other half was enclosed in an argon-filled plastic envelope and analyzed by NRA in the IST facilities at a later time. A summary of the results for all samples is given in table 2. As seen sample #1 shows the highest D retention value, being the only one on which NRA results are above the detection threshold. Contrary to the rest, this sample was not outgassed previous to its exposure to the plasma, and it will not be included in the discussion. Three representative TDS plots are shown in figure 5: Sample #2, $T_{exposure} = 673$ K, bias at −80 V, sample #5, same temperature but at floating potential and sample #6, $T_{exposure} = 403$ K, floating. While the TDS maximum takes place at $T = 900$ K in the two first cases, a clear maximum at 600 K with a second, weaker one at $T > 1000$ K are seen in the sample exposed to lower temperature. Interestingly, the integrated amounts for both curves are very similar, 2.6 and 2.9 in 10^{18} D m^{-2} units respectively, even when a clear deposition of lithium was seen in sample #6 as described above. Furthermore, higher exposure temperatures led to lower retention values for biased samples.

Due to the characteristics of the mass spectrometer used in the analysis of the released gas (MKS Microvision), discrimination between D_2 and He was possible. The corresponding TDS spectra for He, shown in figure 6, exhibit maxima at $T = 900$–1000 K and total doses of up to $1 \times 10^{19}\,m^{-2}$ for biased samples. However a negligible desorption was seen for samples exposed at floating potential, thus suggesting an ion-driven retention process. Remarkably, no He emission lines were detected by OES as seen in figure 2. Although the origin of this helium contamination is not fully understood, the fact that PISCES A was working in

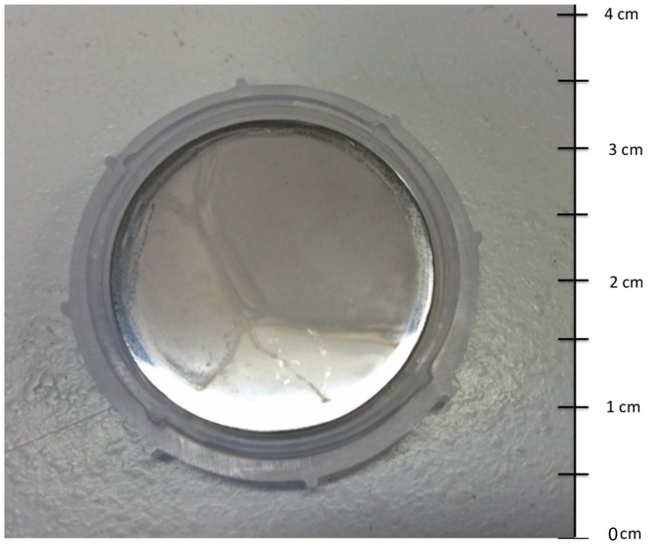

Figure 4. Photograph of sample #6 showing the presence of an inhomogeneous Li film.

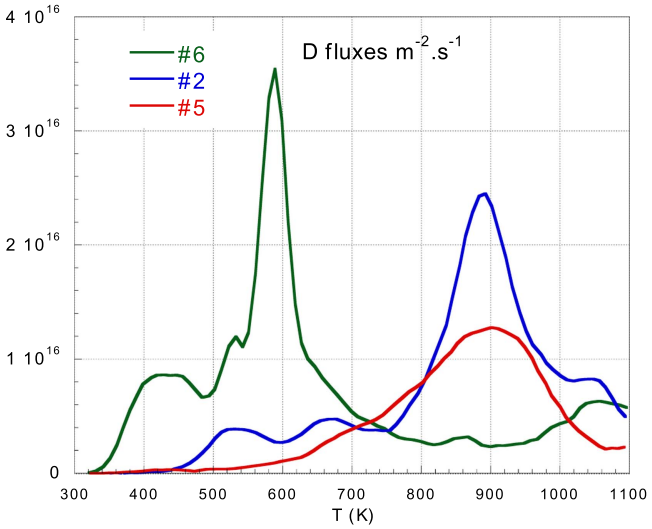

Figure 5. TDS recordings of D_2 desorption for some selected samples. Sample #2, $T_{exposure} = 673$ K, bias at −80 V, sample #5, same temperature but at floating potential and sample #6, $T_{exposure} = 403$ K, floating.

He plasmas prior to the present experiments points to a memory effect of the metallic wall. In fact, a cleaning run on D plasmas performed just after the experimental campaign here described showed no He uptake at the target.

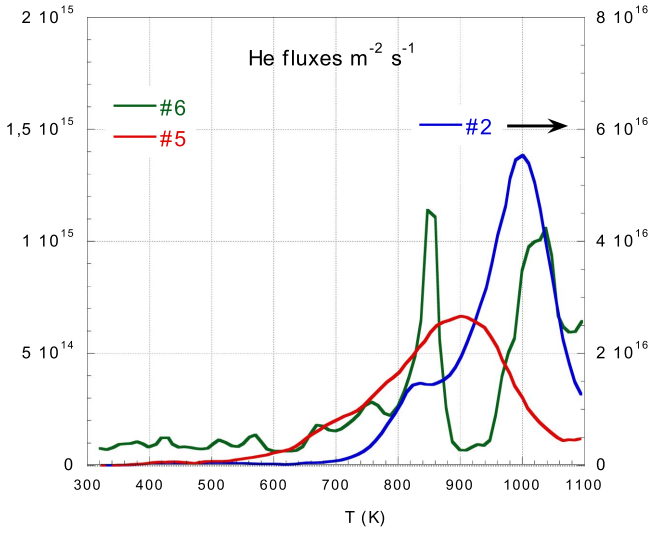

Figure 6. TDS recordings of He desorption for the some selected samples.

The results from NRA support the low D retention values obtained by TDS. No signal above the detection limit of $10^{19}\,\mathrm{D\,m^{-2}}$ was obtained for any of the high temperature samples. An upper limit of $5 \times 10^{18}\,\mathrm{D\,m^{-2}}$ was established for sample #6, the only one with a detectable Li deposition, after integrating the proton emission in order to improve the detection level.

4. Discussion

Previous studies of Li films on W samples exposed to D and He plasmas indicate that a LiD layer develops up to a saturation value at sample temperatures $T < 370\,\mathrm{K}$ [11] and that Li coatings are able to suppress the formation of fuzzy tungsten and provide a self-healing mechanism due to strong redeposition at high fluxes [12]. However these studies were carried out in pre-coated samples, aimed at protecting W surfaces against plasma-induced morphology changes. On the other hand, Baldwin *et al* studied the dynamics of film formation in Be and C seeded plasmas on tungsten samples [13]. Their results indicate that small quantities of these low Z elements may significantly affect the morphology of the W surface and its chemical composition for a given range of temperatures and impurity concentration in the plasma. As the authors point out, the growth of a film on a substrate exposed to a seeded D plasma can be readily described by a balance between the incoming and loss fluxes [14]

$$\mathrm{d}\delta/\mathrm{d}t = (\Gamma_{\mathrm{in}} - \Gamma_{\mathrm{loss}}).\ A_{\mathrm{w}}/(\rho.\ N_{\mathrm{A}}.\ S), \tag{3}$$

where δ is the film thickness, the incoming and loss fluxes are given in at $\mathrm{s^{-1}}$, A_{W} is the atomic weigh (7 for Li), ρ its density, N_{A} Avogadro´s number and S the sample area ($4.9\,\mathrm{cm^2}$ in our case). In a first approach, the incoming flux, Γ_{in}, is given by the content of the plasma in the seeded species and the total impinging particle flux. However in a more realistic situation, the flux of ionized species undergoing prompt redepostion near the target should also be taken into account. For the loss flux, sputtering by plasma ions and self-sputtering together with evaporation and inward diffusion may contribute to the inhibition of film formation [14]. According to the data obtained here, typical values for Γ_{in} are $\sim 2.5 \times 10^{14}\,\mathrm{at\,cm^{-2}\,s^{-1}}$. On the other hand, the evaporative fluxes of lithium at 673 K and 873 K are 4×10^{16} and $2.5\ 10^{19}\,\mathrm{at\,cm^{-2}\,s^{-1}}$ respectively [7]. That means that even without considering the sputtering of Li by D ions, no film growth is expected at the temperatures used in our experiments. However, the mean free path of thermal Li atoms in the D plasma ionized by electron collisions

$$\lambda = v_{\mathrm{Li}}/\langle\sigma v_{\mathrm{e}}\rangle n_{\mathrm{e}} \tag{4}$$

is of the range of 1–0.5 cm ($v_{\mathrm{Li}} \sim 10^5\,\mathrm{cm\,s^{-1}}$, $\langle\sigma v_{\mathrm{e}}\rangle = 8 \times 10^{-8}\,\mathrm{cm^3\,s^{-1}}$, $n_{\mathrm{e}} = (1\text{–}2)10^{12}\,\mathrm{cm^{-3}}$). Therefore, a significant probability of ionization of the evaporated flux near the surface is to be expected. The lithium ions so created will be accelerated by the sheath potential and will impinge on the negatively biased target. Consequently, a high recycling of Li will take place at the target at $T > 673\,\mathrm{K}$ Visual observation of the plasma facing the W target showed indeed an intense red plume although it was not quantitatively characterized.

The situation should significantly change at lower target temperatures due to the exponential dependence of the evaporative flux with temperature. Thus, for 403 K, with Li in the solid state, the evaporation flux is negligible and physical sputtering by D and Li ions (self-sputtering) alone would account for the surface losses. For an average surface density of $1.6 \times 10^{18}\,\mathrm{cm^{-2}}$ and a plasma duration of 1800 s, a total Li flux of $3.6 \times 10^{15}\,\mathrm{s^{-1}}$ is obtained if no losses are considered. This value is higher than that evaluated above from pure geometrical considerations, which are obviously not accurate enough to draw any conclusion about the sputtering efficiency of the plasma under floating target conditions. It should also be noted that a noticeable inhomogeneity on the deposition pattern, as seen in figure 4, will contribute to this discrepancy.

Rather than lithium deposition on the reactor walls, the main concern from the nuclear safety regulation point of view stems from the associated tritium uptake that may take place under routine operation of the device. The results obtained here in the absence of Li film deposition and with a $-80\,\mathrm{V}$ bias are an order of magnitude lower than those reported for pure D plasma exposure of tungsten at the temperatures and plasma conditions here involved, $(1\text{–}2) \times 10^{19}\,\mathrm{m^{-2}}$ [15], and are in the order of those obtained when W is exposed to He contaminated D plasmas [15, 16]. A minimum exposure dose of $5 \times 10^{23}\,\mathrm{m^{-2}}$ of He seems to be required to trigger the retention inhibition through surface bubble formation. As mentioned above, He retention was inferred though TDS analysis of our samples even when no He emission lines were detected in the plasma.

However, not all the results can be explained in terms of He contamination of the plasma. Sample #5 was exposed at floating potential and He retention lower by a factor of 10 compared to biased samples was deduced from TDS. Even so, D retention levels similar to those seen in biased samples were found. Furthermore, sample #6, also at floating potential, developed a lithium film that, being at a temperature

below the melting point of this element, should be prone to hydride formation [17]. Assuming the surface density obtained from NRA for the Li deposit, retention in the form of hydride should lead to values 10^4 higher than measured. While in sample #5 it could be argued that a 1% He contamination would suffice for reaching the required He fluence of $5 \times 10^{23}\,m^{-2}$ for surface bubble formation [16] even at energies or the order of 10 eV, the desorbed amount obtained by TDS, $<10^{17}\,m^{-2}$, is far below the surface density of He associated to the onset of a nano-bubble network development, at $5 \times 10^{20}\,m^{-2}$ [18].

As seen in figure 5, the maxima of the TDS spectra obtained for D outgassing are located at 900 K (sample held at 673 K) and 1000 K (sample at 873 K). High T peaks are missing in the TDS plot for sample #6, exposed at 403 K and covered by a Li film. In this case, a single peak at 600 K is observed. In previous studies, it has been shown that He bubble accumulation at the surface leads to desorption peaks at T between 500 and 600 K [16], an effect not taking place in our case.

Together with the relatively low He surface concentration deduced from TDS in all samples and the lack of He emission in the plasma, all this evidence makes highly questionable the explanation of the TDS results based on the contamination of the plasma by background He.

The single TDS peak at 600 K detected in sample #6 is characteristic of thin lithium film formation [19]. However, the very low amount of retained D precludes hydride formation. In a previous publication [17] Baldwin *et al* found retention values up to $7 \times 10^{24}\,D\,m^{-2}$ on solid Li samples exposed to high flux plasmas. The saturation of the ion range by hydride in D plasma experiments is indeed a common finding for solid Li samples and therefore the retained amount of D should scale with exposed area. The values here reported are quite surprising and we may speculate with the possibility of Li incoming from the plasma leading to the release of D, thus preventing the formation of hydride. The figures shown in table 2 yield a D/Li ratio $<10^{-4}$ for our experimental conditions, even lower than for ITER-like W [15]. This D releasing, or trapping inhibition, mechanism could also be behind the anomalously low retention found on W samples with no Li deposition and it deserves further studies, including microscopic characterization of the exposed surfaces.

The combination of material here addressed aims at simulating the scenario of a reactor working with a Li-based divertor (either Li or LiSn) and a W hot FW. Leakage from the divertor will lead to a Li-containing SOL, with Li/D ratios in the range of the values explored here. Higher energies however are to be expected near the FW of a reactor, their value given by the ion temperature and sheath potential. In a previous work [20] performed in a GD plasma, it was found that for Li ion energies of several hundred eVs no D retention associated to Li ion bombardment took place as expected from the very low range of implantation of Li on W. Based on these facts, it seems very unlikely that D retention of the FW of a reactor at typical temperatures equal or higher than those used here becomes an issue, as it was found for carbon-based divertor materials.

5. Summary and conclusions

The interaction between lithium-seeded (1%–2%) deuterium plasmas and tungsten targets has been studied in the PISCES-A divertor plasma simulator at sample temperatures between 403 and 873 K and total fluence of $5 \times 10^{25}\,m^{-2}$. The main findings are:

- No macroscopic Li film developed on samples kept at 673–873 K.
- A layer with thickness consistent with the expected lithium content of the plasma and a negligible evaporation at the target was found in a sample kept at 403 K.
- D retention values lower than those seen in pure D plasmas by a factor of 10 were recorded for W samples without any film coverage.
- A ratio of $D/Li < 10^{-4}$ was deduced for the sample kept at low temperature.

Acknowledgments

The authors are indebted to the Eurofusion PFC and DTT teams on liquid metal research for fruitful discussions and suggestions. This work was partially financed by the Spanish 'Ministry of Economy and Competitivity' under project ENE2014-58918-R. This work has been carried out within the framework of the Eurofusion Consortium and has received funding from the Erratum research and training program 2014–2018 under grant agreement No 633053. The views and opinions expressed herein do not necessarily reflect those of the European Commission.

References

[1] Abdou M 2001 *Fusion Eng. Des.* **54** 181
[2] Nygren R and Tabarés F L 2016 *Nucl. Mater. Ener.* **9** 6
[3] Mirnov S V *et al* 2011 *Nucl. Fusion* **51** 073044
[4] Tabarés F L *et al* 2017 Reactor plasma facing component designs based on liquid metal concepts supported in porous systems *Nucl. Fusion* **57** 016029
[5] Roth J *et al* 2008 *Plasma Phys. Control. Fusion* **50** 103001
[6] Goebel D M *et al* 1984 *J. Nucl. Mater.* **121** 277
[7] Kallenbach A *et al* 2013 *Plasma Phys. Control. Fusion* **55** 124041
[8] Mills A F 1999 *Heat Transfer* 2nd edn (Upper Saddle River, NJ: Prentice Hall, Inc)
[9] Whyte D G *et al* 1999 *J. Vac. Sci. Technol.* A **17** 2713
[10] Gasparyan Y M *et al* 2016 *Fusion Eng. Des.* accepted (https://doi.org/10.1016/j.fusengdes.2016.07.025)
[11] Li C *et al* 2014 *Fusion Eng. Des.* **89** 949
[12] Neff A L *et al* 2015 *J. Nucl. Mater.* **463** 1147
[13] Baldwin M J *et al* 2009 *J. Nucl. Mater.* **390–391** 886

[14] Baldwin M J *et al* 2007 *J. Nucl. Mater.* **363–365** 1179
[15] Baldwin M J *et al* 2011 *Nucl. Fusion* **51** 103021
[16] Lee H T *et al* 2007 *J. Nucl. Mater.* **360** 196
[17] Baldwin M M J *et al* 2002 *Nucl. Fusion* **42** 1318
[18] Iwakiri H *et al* 2002 *J. Nucl. Mater.* **307–311** 135
[19] Skinner C *et al* 2013 *J. Nucl. Mater.* **438** S647
[20] de Castro A *et al* 2016 *Fusion Eng. Des.* accepted (https://doi.org/10.1016/j.fusengdes.2016.10.011)